Energy-dispersive measurements of individual $K\beta$ x-ray relative transition probabilities in heavy elements

J. A. Maxwell and J. L. Campbell
Guelph-Waterloo Program for Graduate Work in Physics, University of Guelph, Guelph, Ontario N1G 2W1, Canada
(Received 25 August 1983)

The relative transition probabilities $K\beta_3/K\beta_1$, $K\beta_2/K\beta_1$, $KO_{23}/K\beta_1$, $KP_{23}/K\beta_1$, $K\beta_5/K\beta_1$, and $K\beta_4/K\beta_1$ are measured by Ge spectroscopy for the atoms having $Z=70$, 78, 82, and 92. In contrast to previous data, the results exhibit smooth Z dependences and agree closely with Scofield's relativistic Hartree-Fock calculations. A tentative observation of the KM_1 transition is reported.

I. INTRODUCTION

The history of measurement of relative transition probabilities and x-ray widths for the K shell spans several decades. Prior to 1960 systematic measurements were made by various workers using crystal diffraction techniques for point-by-point recording of x-ray spectra. An early example is the extensive study by Beckman,[1] who recorded the K x-ray spectra resulting from bombardment of thick targets by energetic electrons. Around 1970 the appearance of relativistic Hartree-Slater (RHS) computations[2] of decay rates stimulated further wavelength dispersive studies using other excitation techniques for thick targets. The advent of lithium-drifted Ge and Si energy-dispersive detectors in the late 1960's resulted in a flurry of measurements, in the period 1969—1973, of relative probabilities for the restricted set of major K lines and groups of lines that could be resolved by these devices. Their order-of-magnitude poorer resolving power was compensated by various advantages, e.g., their high efficiency and their ability to record the entire K-series spectrum in a single measurement. Perhaps the most important aspect was that very small quantities (~ 1 μCi) of x-ray emitting radionuclides could now be used as spectral sources, thus eliminating the serious photon attenuation problems inherent in the thick sources used in wavelength-dispersive work. References to the Si(Li) and Ge(Li) work are listed in a comprehensive review by Salem *et al.*,[3] who present fits to various measured x-ray line and group ratios as functions of the atomic number Z. This review pointed out well-defined discrepancies between the gross $K\beta/K\alpha$ ratios and the RHS predictions. The discrepancies disappeared when Scofield's relativistic Hartree-Fock (RHF) calculations[4] were used; in these, proper account was taken for the first time of the difference between the single-particle wave functions in the initial and final states, and the resulting exchange contributions were included in the decay rates.

Recently a few measurements using the current "state of the art" in both wavelength- and energy-dispersive spectroscopy have been reported. Campbell and Schulte[5] made the first energy-dispersive measurements of $K\alpha$ linewidths, using least-squares fitting of Voigtian line shapes to extract the desired information from Ge(Li) spectra; the widths agreed much better with RHF values than tabulated widths based on previous experimental work. Both Barreau *et al.*[6] and Kessler *et al.*[7] reported very precise wavelength-dispersive studies, which further improved the agreement of $K\alpha$ and $K\beta$ linewidths with theory. Campbell and Schulte presented $K\alpha_2/K\alpha_1$ ratios, claiming 1% precision, and Barreau *et al.* presented relative transition probabilities for several K lines.

Examination of all the data for medium-to-high Z reveals that, for transitions from the $M,N,O,\ldots$ shells to the K shell, only a minority of reported experiments actually contribute to a critical test of Scofield's RHF theory.[4] Since the theoretical values are widely used, e.g., in atomic inner-shell physics and in elemental analysis by x-ray emission [x-ray fluorescence (XRF), proton-induced x-ray emission (PIXE), etc.] critical testing is very desirable. In this paper we examine the available data and report measurements of the relative transition probabilities for 8—9 $K\beta$ lines in atoms of high Z; these were obtained by an extension of the techniques used previously for the $K\alpha$ line.[5]

The reader should note that the term "intensity ratio" for two x-ray lines (energies E_1,E_2) refers to the quantity $\lambda_1 E_1/\lambda_2 E_2$ and is not precisely equal to the ratio λ_1/λ_2 of transition probabilities. However, in the literature intensity ratio often is used to denote λ_1/λ_2. We shall use the abbreviation RTP to denote ratio of transition probabilities.

II. REVIEW OF PREVIOUS RESULTS

Figure 1 is typical of the K x-ray spectra of heavy elements recorded with a Ge detector. The two KL components $K\alpha_2$ and $K\alpha_1$ are partially or wholly resolved, but the many KM, KN, KO, and KP lines overlap in the $K\beta$ region. For these reasons almost all published energy-dispersive work provides only the $K\alpha_2/K\alpha_1$ RTP and the ratios of the gross $K\beta'_1$ and $K\beta'_2$ probabilities relative to the $K\alpha$ probability; the few exceptions will be discussed later. In diffraction spectroscopy the $K\beta'_1$ group is partially or wholly resolved into the strong $K\beta_3$ and $K\beta_1$ dipole lines and the weak $K\beta_5$ doublet which is of electric quadrupole nature; the $K\beta'_2$ group displays structure from which curve-fitting procedures can extract the intensities of the $K\beta_2$, $KO_{2,3}$, and $K\beta_4$ (quadrupole doublet) transi-

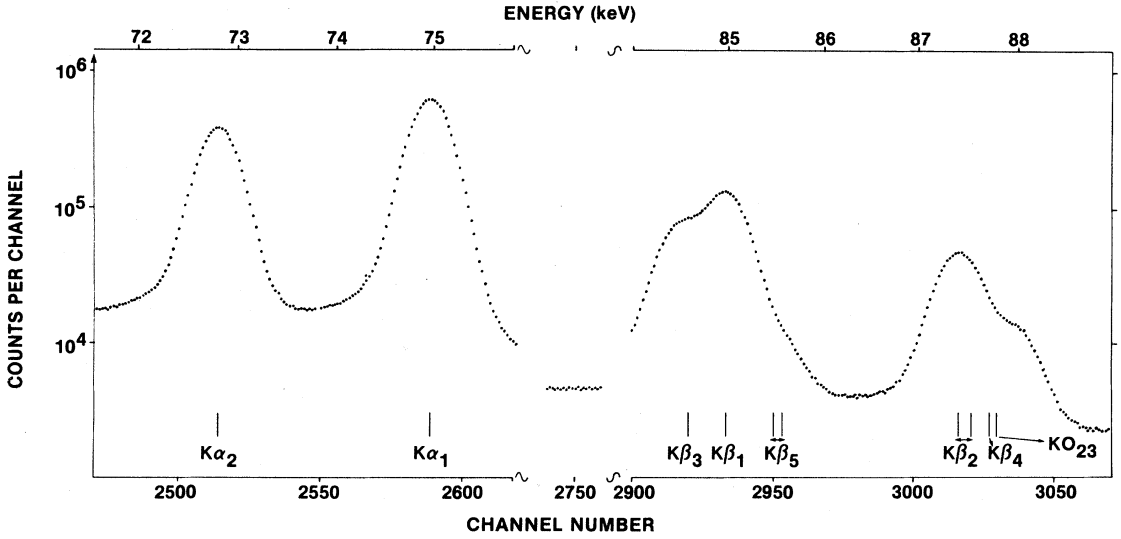

FIG. 1. K x-ray spectrum of lead, from a ^{207}Bi radionuclide source, recorded with a Ge detector.

tions. Table I summarizes the nomenclature.

We now examine in detail the available data at high Z, where the experimental accuracy should be best due to the greater energy or wavelength separation of the various lines.

There is a vast quantity of data on the gross $K\beta/K\alpha$ and on the $K\alpha_2/K\alpha_1$ (KL_2/KL_3) relative transition probabilities, and these are summarized in figures given by Salem *et al.*[3] While there is a large scatter, there is so much information that Salem *et al.*'s claim that their "best fits" are accurate to about 2% is quite acceptable. Moreover, the agreement between the best fits and RHF predictions is on the order of 1%. In trying to evaluate $K\beta$ measurements in any given publication we find it extremely useful to compare the accompanying $K\alpha_2/K\alpha_1$ measurements with the Salem *et al.* best fit; this provides a valuable rejection criterion for $K\beta$ data.

This paper focuses on the $K\beta$ group, where matters are less satisfactory and where more definitive measurements appear to be needed. Only a handful of the many reported measurements provide RTP's for individual $K\beta$ components, e.g., $K\beta_3/K\beta_1$, $K\beta_5/K\beta_1$, etc.

Figure 2 adds the more recent data to the $K\beta_3/K\beta_1$ data collected in a similar figure by Salem *el al.*[3] in their review. The curve representing the best fit to data published before 1974 diverges from the RHF prediction with increasing Z. About a quarter of the data points used by Salem *et al.* are from the venerable wavelength-dispersive work of Beckman;[1] the same series of measurements provided $K\alpha_2/K\alpha_1$ ratios which fell some 14% below both the theory and the Salem *et al.* fit—indeed they had to be excluded from that fit. Beckman had to make large corrections for target self-absorption (11—21%) and crystal reflection efficiency (29%) and the $K\alpha_2/K\alpha_1$ results suggest that the corrections were not accurate. Schult's[8] wavelength-dispersive work using K x rays arising from neutron capture in thick targets also involved large absorption effects which could not be calculated with high accuracy. Salem *et al.*[9] reported a set of $K\beta_3/K\beta_1$ data using γ rays to fluoresce targets, and, although the data

TABLE I. X-ray transition nomenclature.

KL_2	$K\alpha_2$	$K\alpha$
KL_3	$K\alpha_1$	
KM_2	$K\beta_3$	$K\beta_1'$
KM_3	$K\beta_1$	
KM_4	$K\beta_5$	
KM_5		
KN_2	$K\beta_2$	$K\beta_2'$
KN_3	$K\beta_4$	
$KN_{4,5}$		
KO_{23}		

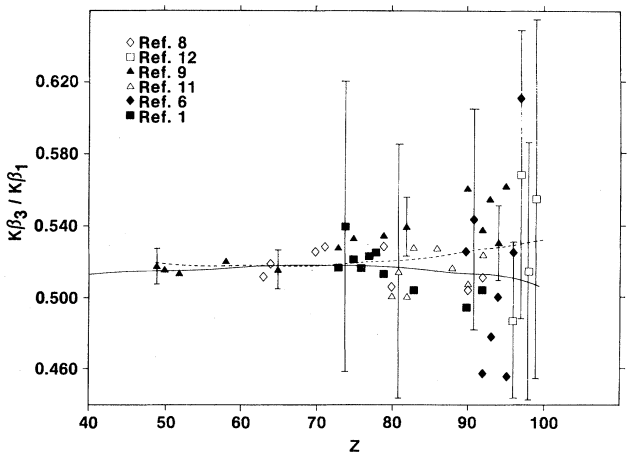

FIG. 2. Comparison of measured $K\beta_3/K\beta_1$ relative transition probabilities with the 1974 best fit of Salem *et al.* (Ref. 3) (dashed curve) and the relativistic Hartree-Fock calculations of Scofield (Ref. 4) (solid curve).

lie above both theory and best fit in Fig. 2, they receive strong support from the agreement of the same group's $K\alpha_2/K\alpha_1$ data[10] with theory. The only other wavelength-dispersive data in Fig. 2 are from Barreau *et al.*'s recent study[6] of K x-ray spectra from (n,γ) reactions on actinides; these data scatter widely, while the companion $K\alpha_2/K\alpha_1$ data follow the theory although with a similar large scatter.

Only two energy-dispersive studies present RTP's for individual $K\beta$ lines as distinct from gross groupings. de Pinho[11] reported various ratios but gave no indication as to how the $K\beta'_1$ multiplet was unfolded or as to how his uncertainties were arrived at; however, his $K\alpha_2/K\alpha_1$ data are uniformly 2% below theory and so there is no reason to exclude his $K\beta_3/K\beta_1$ data from Fig. 2. Dittner and Bemis[12] also gave little detail concerning data analysis and while their $K\alpha_2/K\alpha_1$ results agree closely with theory their $K\beta_3/K\beta_1$ data scatter widely.

Figure 2 then contains data points from four wavelength-dispersive studies and two energy-dispersive studies, in addition to the fit of Salem *et al.*[3] to all data published before 1974. The data of Salem *et al.*[9] show a strong uniform divergence from theory as a function of Z.

Data on RTP's involving components from the $K\beta'_2$ series are very sparse indeed. For KN_{23}/KM_3, KO_{23}/KM_3, KM_{45}/KM_3, and KN_{45}/KM_3 the only wavelength-dispersive data are those of Beckman[1] and of Schult,[8] and we have already indicated that these may be inaccurate due to absorption problems. The Salem *et al.*[3] review indicates that these follow the theory within an uncertainty of perhaps $\pm 10\%$. Only de Pinho[11] has reported energy-dispersive work, and as already pointed out, no detail was given regarding peak unfolding, although it is likely that a graphical method was used.

One is thus forced to the conclusion that despite the plenitude of data on gross x-ray groups and on the $K\alpha_2/K\alpha_1$ RTP, there is currently little reliable information on the RTP's for x-ray transitions from the M, N, O, and P shells to an initial K vacancy.

III. OBJECTIVES

Measurements of K x-ray spectra using radionuclide sources and Ge spectrometers are free of self-absorption effects and the only experimental corrections are easily determined corrections of a few percent for relative detector efficiency. Since we had already reported Ge(Li) measurements of the $K\alpha_2/K\alpha_1$ RTP that had $\sim 1\%$ precision and which agreed with RHF theory at the 1% level, it was decided to extend the techniques used there to a study of $K\beta$ spectra in atoms of $70 \leq Z \leq 92$. It was not felt necessary to measure at a large number of Z values since the theoretical predictions have only modest Z dependence. Accordingly, Z values of 70, 78, 82, and 92 were chosen to span the region effectively.

IV. EXPERIMENTAL DETAIL

The K x-rays were obtained from radionuclide sources of ^{171}Tm, ^{195}Au, ^{207}Bi, and ^{235}Np. The first two were prepared by drying droplets on 0.125-mm Mylar and the third similarly using 0.05-mm beryllium. The ^{235}Np source was prepared by K. M. Glover and B. Whittaker of the United Kingdom Atomic Energy Research Establishment (Harwell Laboratory); it was also on a Mylar backing.

Spectra were recorded on an intrinsic planar Ge detector of dimensions 10-mm depth $\times$ 10-mm diam (Aptec Inc.). The energy resolution of this device at 84 keV, in the center of the energy region of interest, was 435 eV [full width at half maximum (FWHM)]. Counting rates were held below 100 s^{-1} and both a pulse pile-up inspector (in the Ortec 572 amplifier) and a locally made rise-time inspector were used to prevent any distorted pulses being accepted by the 4096-channel analog-to-digital converter (Nuclear Data 2200). The latter had a specially modified input circuit to improve the differential nonlinearity; this was measured by recording the spectrum from a Berkeley Nucleonics pulser which provided a flat pulse height distribution by using a linear ramp. The mean channel width varied by less than 0.1% across the energy region used. In recording the K x-ray spectra, a digital stabilizer was set on the $K\alpha_1$ line. The total number of counts in the $K\beta$ spectral region ranged from about 9×10^6 for uranium to 40×10^6 in the lead case.

To ensure that the resolution function of the detector was adequately known, spectra were also recorded for a set of γ rays spanning the energy region of interest. These were prepared from sources of ^{241}Am, ^{170}Tm, ^{171}Tm, ^{153}Gd, and ^{57}Co in precisely the same manner as the x-ray sources. For each peak of interest about 5×10^6 counts were accumulated.

The absolute detection efficiency was measured using a set of radionuclide standards. These included ^{241}Am (Physische-Technische-Bundesanstalt, Germany), ^{57}Co and ^{133}Ba (Atomic Energy of Canada Ltd.), and the mixed standard 4275-170 supplied by the U. S. National Bureau of Standards; lines from ^{154}Eu and ^{155}Eu were used in the last case. The resulting curve is shown in Fig. 3, where the data points lie on a smooth line. These data were used to correct the intensities of the various $K\beta$ x-ray lines of interest for the change in efficiency across the relevant few keV energy interval. The corrections were less than 6% and are accurate to about one-tenth of that.

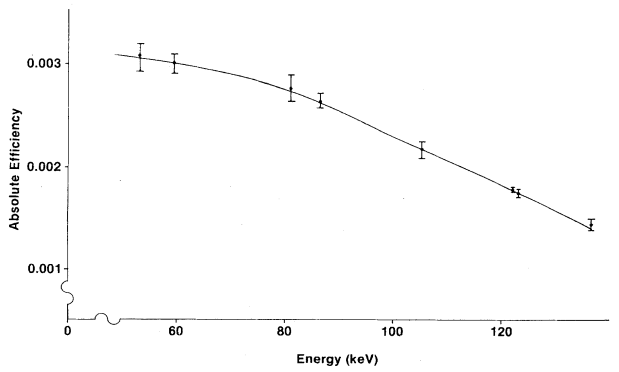

FIG. 3. Measured absolute efficiency of Ge detector. The error bars represent 99% confidence level.

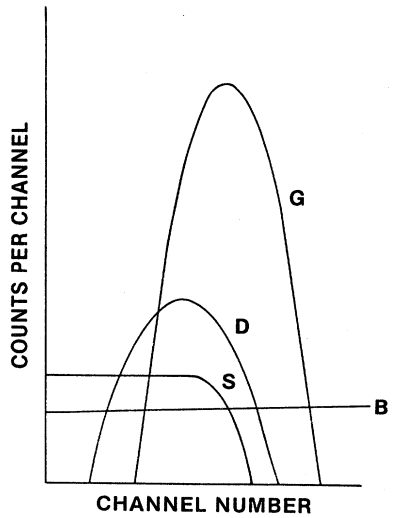

FIG. 4. Additive analytic components of spectral peak due to monoenergetic photons.

V. DATA ANALYSIS

Each γ-ray peak was fitted with the resolution function[5] that was used (for a different detector) in our previous work on $K\alpha$ spectra. It is

$$F(x)=B(x)+G(x)+S(x)+D(x) \tag{1}$$

and the four additive components are shown schematically in Fig. 4. The main Gaussian component

$$G(x)=H_G\exp\left[\frac{-(x-x_0)^2}{2\sigma^2}\right] \tag{2}$$

is the shape expected in a perfect detector for a peak centered at x_0 with height H_G and FWHM 2.35σ. Detector imperfections result in a flat low-energy shelf and in an exponential low-energy tail which, when convoluted with the basic Gaussian response, yield the components

$$S(x)=\tfrac{1}{2}H_S\left[1-\mathrm{erf}\left[\frac{x_0-x}{\sigma\sqrt{2}}\right]\right] \tag{3}$$

and

$$D(x)=\tfrac{1}{2}H_D\exp\left[\frac{x-x_0}{\beta}\right]\mathrm{erfc}\left[\frac{x-x_0}{\sigma\sqrt{2}}+\frac{\sigma}{\beta\sqrt{2}}\right] \tag{4}$$

in which H_S and H_D are heights and β is the slope parameter of the tail. Finally, $B(x)$ is a linear background,

$$B(x)=ax+b\ . \tag{5}$$

The eight parameters $a,b,H_G,\sigma,x_0,H_S,H_D,\beta$ are determined using a nonlinear least-squares algorithm[13] to minimize the χ square.

The reduced χ-squared values for the six peaks used are collected in Table II. In each case the region fitted spanned some 250 channels centered on the peak, whose FWHM was typically 10—15 channels. It would be unrealistic to expect χ_r^2 values close to 1.0 since we accumulated unusually high intensities and in the presence of systematic errors of the model χ_r^2 grows in proportion to intensity.[14]

TABLE II. Reduced χ^2 for fits to monoenergetic γ-ray spectra.

Energy (keV)	Nuclide	χ_r^2
59.54	^{241}Am	1.16
66.72	^{171}Tm	1.20
84.26	^{170}Tm	1.37
97.43	^{153}Gd	1.60
103.18	^{153}Gd	1.44
122.10	^{57}Co	1.56

In our previous work we found it necessary to use two tails, viz., $D_1(x)$ and $D_2(x)$ of very different slope. Our present detector's response is superior to that of the previous one and addition of a second tail to the model does not improve the quality of the fits. The function of Eq. (1) is clearly appropriate.

In fitting the $K\beta$ x-ray spectrum of a particular element, account must be taken of the intrinsic Lorentzian energy distribution of each component. In all previous energy-dispersive work on the $K\alpha$ and $K\beta$ series this intrinsic line shape was neglected. The Lorentzian energy distribution is

$$L(x)=\frac{\Gamma/2\pi}{(x-x_0)^2+(\Gamma/2)^2}\ , \tag{6}$$

where Γ is the width of the line. If the K vacancy is filled from the A_i subshell ($A_i=M_2$, M_3, etc.), then the x-ray width is the sum of the K and A_i level widths, i.e.,

$$\Gamma=\Gamma(K)+\Gamma(A_i)\ . \tag{7}$$

This intrinsic line shape has been incorporated into Eq. (1) simply by replacing the Gaussian $G(x)$ by the Voigt function $V(x)$ which is the analytic convolution of $G(x)$ with $L(x)$; the Voigt function is evaluated here by piecewise series approximations due to Armstrong.[15] In its original form, using double-precision arithmetic, Armstrong's code is accurate to 1—2 parts in 10^6; however, for the specific application to our spectra, where $\Gamma/\sigma\simeq 0.2$—0.6, we find that use of single precision causes negligible change in the results. In principle, the minor components $D(x)$ and $S(x)$ should also be convoluted with $L(x)$. However, in the peak region ($x_0-3\sigma\le x_0\le x_0+3\sigma$) these account for only about 4% of the total area, and so we feel justified in restricting the convolution to the more easily handled Gaussian component.

The typical $K\beta$ spectrum at high Z is modeled by 8 or 9 components, as listed in Table I. The KN_4 and KN_5 lines are very close in energy compared to the detector resolution and are considered as a single line; the same applies to the $KO_{2,3}$ doublet. Further simplification along these lines could have been achieved by coalescing the KM_4 and KM_5 lines into a single $K\beta_5$ line, and the KN_2 and KN_3 lines into a single $K\beta_2$ line; however, this worsened the

quality of the fits significantly and was therefore rejected.

Each of the components listed in Table I is represented separately by Eq. (1), but the number of variable parameters is restricted by the following constraints.

(i) Since the component energies E are accurately known,[16] and since the electronic system has been shown to be highly linear, the 8 (or 9) Voigtian centroids x_0 are obtained from the equation

$$x_0 = C_1 + C_2 E \ , \tag{8}$$

the number of position variables thereby being reduced to 2, viz., C_1 and C_2. The energy E is in keV.

(ii) The resolution linewidth $\sigma(E)$ of a Ge spectrometer is given[17] by

$$\sigma = (\sigma_n^2 + F\epsilon E)^{1/2} \tag{9}$$

where σ_n^2 is the system noise, and $F\epsilon E$ the statistical fluctuation in pulse size, both in units keV^2; ϵ is the energy per ion pair (2.96×10^{-3} keV) and F the Fano factor, whose value is most probably about 0.1 or a little less.[17] We determined $F\epsilon$ by least-squares fitting (9) to the σ vs E data obtained from the γ-ray fits; the resulting value of 0.30 eV was in good agreement with the expected value based on the numbers given above.

Transformation of Eq. (9) from energy units into channel number units then gives

$$\sigma = (C_3 + C_4 E)^{1/2} \ , \tag{10}$$

where

$$C_4 = F\epsilon C_2^2 \ . \tag{11}$$

If both C_3 and C_4 are allowed to vary in the K x-ray fits, they have large associated uncertainties, because σ only changes slightly across the $K\beta$ group. These uncertainties cause spuriously high uncertainties in derived peak areas. In practice, therefore, only C_3 was allowed to vary, C_4 being set by Eq. (11).

(iii) The 8 (or 9) spectral lines all have different intrinsic widths Γ. However, these Γ values are all dominated by the common Γ_K (40–100 eV) and the differences are due entirely to the outer subshell width which is only a few percent of Γ_K. It seemed reasonable therefore to employ a single, common Γ value. This was estimated for each Z of interest using the tables of Krause and Oliver.[18] In the fitting procedure Γ was held at this value. Fitting runs with Γ held at values 1–2% greater or smaller demonstrated an insenstivity to variations at this, the permissible, level.

(iv) The results of the nuclear γ-ray fits show that the parameters H_D and β which describe the non-Gaussian feature of the resolution function vary smoothly with energy. However, the energy-dependence is small and can certainly be neglected within either the $K\beta_1'$ or the $K\beta_2'$ group. We therefore used four parameters to describe the distortion. For $K\beta_1'$ these were $h_1 = H_D/H_G$ and $s_1 = \beta/\sigma$, with h_1 and s_1 being common to the four $K\beta_1'$ components; a similar arrangement in terms of variable parameters h_2 and s_2 described $K\beta_2'$. The step height H_S is to some extent a function of the choice of fitting region and for the γ rays it had no well-defined energy dependence; hence for the x rays one variable parameter $h_S = H_S/H_G$ is used, common to all components.

TABLE III. Details of fits to $K\beta$ x-ray spectra.

Z	Nuclide	χ_r^2	Number of counts	$\langle\Delta^2\rangle_{av}^{1/2}$ [a]
70	^{171}Tm	1.18	1.29×10^7	3.9×10^{-6}
78	^{195}Au	1.40	1.40×10^7	9.7×10^{-6}
82	^{207}Pb	1.41	3.07×10^7	6.0×10^{-6}
92	^{235}Np	2.30	9.2×10^6	5.1×10^{-5}
		(1.82)	9.2×10^6	3.4×10^{-5}

[a] $\langle\Delta^2\rangle_{av}^{1/2}$ is equal to $d(\chi_r^2-1)/I$, where d is the number of degrees of freedom and I the integrated spectral intensity.

The total number of parameters set free to vary in the nonlinear least-squares fitting routine was thus 18 (or 19), comprising 8 (or 9) line heights, 2 position parameters, and 1 width parameter (C_1, C_2, C_3), five peak distortion parameters and two background parameters. We have discussed these in some detail since the adequacy of the fitting technique is central to our effort to provide a more critical test of Scofield's predictions than the previous experimental work. The actual fitting was done on a Digital Equipment Corporation MINC 11/23 computer.

VI. RESULTS

The χ_r^2 values for the $K\beta$ x-ray fits are collected in Table III, along with values of the quantity $\langle\Delta^2\rangle_{av}^{1/2}$ suggested by Sekine and Baba[19] and by Campbell[14] as a goodness-of-fit indicator that is independent of the overall number of counts. For $Z=70$, 78, and 82 the fits are excellent; Fig. 5 shows the residues in the $Z=82$ case and no systematic tendencies are apparent. The slightly poorer fit at $Z=92$ may be partly due to minor electronic instabilities during the 10 day measurement that was made necessary by the low K x-ray intensity per decay of ^{235}Np ($\sim$2%); a second cause will be discussed later.

The efficiency-corrected relative transition probabilities are collected in Table IV. The associated uncertainties are derived from the diagonal elements of the error matrix generated by the fitting procedure. The question immediately arises as to whether these results and the correspond-

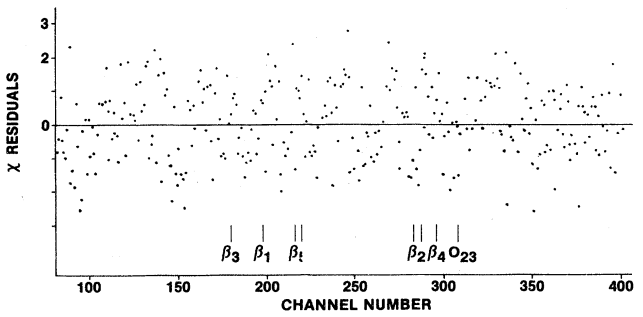

FIG. 5. Residue after fitting the lead $K\beta$ spectrum with eight Voigt functions.

TABLE IV. Relative transition probabilities; E denotes the experimental results; RHS and RHF denote predictions of relativistic Hartree-Slater and Hartree-Fock calculations by Scofield (Refs. 2 and 4).

		$\frac{K\beta_3}{K\beta_1}$	$\frac{K\beta_2}{K\beta_1}$	$\frac{KO_{23}}{K\beta_1}$	$\frac{KP_{2,3}}{K\beta_1}$	$\frac{K\beta_5}{K\beta_1}$	$\frac{K\beta_4}{K\beta_1}$[a]	$\frac{KN_2}{KN_3}$	$\frac{KM_4}{KM_5}$
70	E	0.5152	0.3441	0.0497		0.0279	0.0135		
		±0.0035	±0.0070	±0.0006		±0.0026	±0.0015		
	RHS	0.5175	0.3380	0.0421		0.0224	0.0052		
	RHF	0.5174	0.3488	0.0444					
78	E	0.5119	0.3647	0.0686		0.0345	0.0067		
		±0.0014	±0.0102	±0.0003		±0.0012	±0.0008		
	RHS	0.5172	0.3557	0.0596		0.0282	0.0072		
	RHF	0.5171	0.3676	0.0618					
82	E	0.5124	0.3764	0.0784		0.0412	0.0131	0.513	0.775
		±0.0011	±0.0025	±0.0002		±0.0012	±0.0008	±0.008	±0.047
	RHS	0.5164	0.3650	0.0691		0.0311	0.0083	0.509	0.826
	RHF	0.5158	0.3776	0.0721				0.505	
92	E	0.5080	0.4102	0.1047	0.0196	0.0376	0.0150	0.490	0.824
		±0.0007	±0.0008	±0.0003	±0.0005	±0.0004	±0.0004	±0.002	±0.021
	RHS	0.512	0.387	0.0919	0.0154	0.0383	0.0113	0.494	0.877
	RHF	0.512	0.399	0.0949	0.0174			0.491	

[a]See comments in text on validity of these data.

ing χ^2 values are unique or depend upon the starting parameters of the fitting procedure. This was investigated by varying the starting parameters in several fits to the two cases $Z=70$ and $Z=92$. At $Z=70$ three fits were done; each reached a χ-squared value of 1.20. At $Z=92$, five fits were done, with the resulting χ-squared values ranging from 2.26 to 2.55. Table V summarizes the variations in relative transition probabilities generated by these replicate fits. At $Z=70$ the spreads in the various transition probabilities relative to $K\beta_1$ are within the uncertainties given in Table IV, with the exception of the $K\beta_4/K\beta_1$ case; since $K\beta_4$ is the weakest line in the series, contributing under 1% of the overall $K\beta$ intensity, it is not surprising that the fitted $K\beta_4/K\beta_1$ ratio appears untrustworthy. At $Z=92$, the spread in the five $K\beta_4/K\beta_1$ results was again somewhat larger than the uncertainty given by the program, while other ratios relative to $K\beta_1$ had spreads that were quite acceptable. This analysis of reproducibility versus "internal error" appears to indicate that of the ratios relative to $K\beta_1$, only the $K\beta_4/K\beta_1$ emerges with results that appear to be untrustworthy.

The $K\beta_3/K\beta_1$ RTP's are plotted in Fig. 6 along with the RHF prediction. The decrease in uncertainty with increasing Z is striking, although to be expected. The results lie uniformly about 1% below theory but this difference is not felt to be significant. The monotonic Z dependence of our data is to be compared with the scatter within previous data sets, illustrated in Fig. 2. The other dipole transition ratios also vary smoothly with Z (see Table IV). As shown in Fig. 7 the previous $K\beta_2/K\beta_1$ data follow Z dependences which are very different from the Hartree-Slater and the Hartree-Fock predictions. The present data favor the RHF rather than the RHS curve, confirming the importance of the overlap and exchange effects that have been widely demonstrated in work on the gross $K\beta/K\alpha$ RTP (Ref. 4).

The ratios of the two quadrupole doublets $K\beta_5$ and $K\beta_4$ to the main $K\beta_1$ dipole probability differ considerably from theory at $Z=70$, but the discrepancy diminishes with increasing Z. These two transitions account for less than 5% of the total $K\beta$ intensity of our spectra, and both overlap with much stronger lines (see Fig. 1). It may therefore be unrealistic to expect the fitting procedure to generate accurate results in these cases.

TABLE V. Spreads caused by variation of starting parameters.

RTP	$Z=70$	$Z=92$
$K\beta_3/K\beta_1$	±0.1%	±0.03%
$K\beta_2/K\beta_1$	±0.15%	±0.16%
$K\beta_5/K\beta_1$	±1.3%	±0.25%
$K\beta_4/K\beta_1$	±60%	±4.1%
KN_2/KN_3	±24%	±3.7%
KM_4/KM_5	±27%	±1.0%

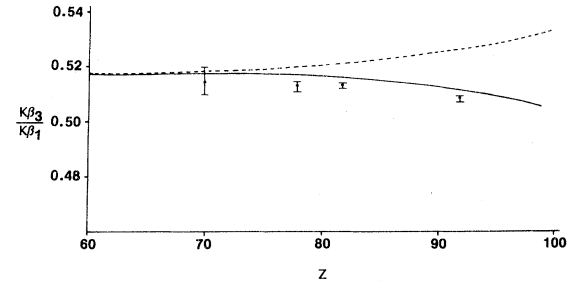

FIG. 6. Comparison between the present results for the $K\beta_3/K\beta_1$ relative transition probabilities and the RHF predictions (Ref. 4). The error bars represent ±1 standard deviation as given by the error matrix generated in the least-squares fit. The solid curve is the RHF theory and the dashed curve the Salem *et al.* fit.

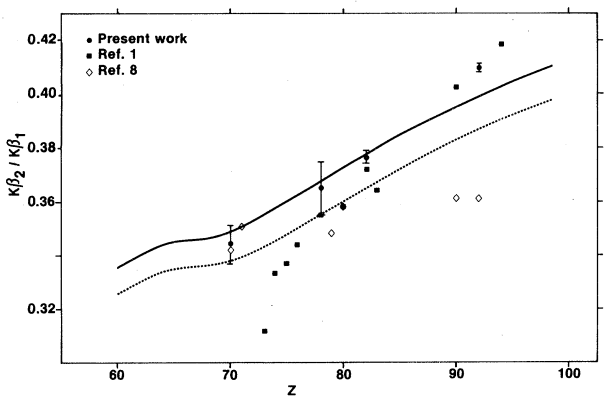

FIG. 7. Comparison of measured $K\beta_2/K\beta_1$ relative transition probabilities with the relativistic Hartree-Slater (dashed curve) and Hartree-Fock (solid curve) predictions of Scofield (Ref. 4).

It would be equally unrealistic to expect useful results for the KN_2/KN_3 and KM_4/KM_5 ratios since the spacing of the members of each of these doublets is much less than the detector resolution. However, given the close agreement with RHF theory of the intrashell RTP's $K\alpha_2/K\alpha_1$ (Ref. 5) and $K\beta_3/K\beta_1$ (present work), it seems reasonable to expect that the RHF predictions for KM_4/KM_5 and KN_2/KN_3 should also be accurate. As noted earlier our results for these ratios at $Z<82$ were not unique. However, for $Z=82$ and 92 the agreement with theory is remarkably good. We regard this observation as lending strong support to our various RTP's relative to $K\beta_1$ at $Z=82$ and 92.

Finally we return to the question of the χ_r^2 value at $Z=92$, which at 2.3 is larger than in the other three cases. The residue here showed a small peak on the left side of the $K\beta_3$ line. This was reminiscent of our original observation[5] of the l-forbidden $K\alpha_3$ line via a finite residue in fits of the $K\alpha$ doublet. A further line, corresponding to the l-forbidden KM_1 transition was therefore added to the model. The χ_r^2 dropped to 1.82 and the KM_1/KM_3 relative transition probability was $\sim 6\times 10^{-3}$ which is of the order of Scofield's RHS prediction[20] of 3.3×10^{-3}. This identification must be regarded as tentative. A definitive test requires much improved counting statistics, which are not economically feasible for ^{235}Np. Measurements on other *trans*-uranic atoms might resolve this intriguing point, and further refine the precision of the various relative transition probabilities.

VII. CONCLUSIONS

We have described the first energy-dispersive experiments which effectively resolve all the significant components of the $K\beta$ x-ray series. In view of our need to interpret the results of the fitting procedure, which is quite complex, with considerable care, it is doubtful that any of the previous Ge(Li) results can be regarded as reliable. We have drawn attention to possible systematic errors in wavelength-dispersive data. The present data therefore provide a unique critical test of Scofield's RHF transition probabilities for M, N, O, and P shells to the K shell. Further work at $Z>92$ would refine this test and shed light on the possible observation of the l-forbidden KM_1 line.

ACKNOWLEDGMENTS

This work was supported by the Natural Sciences and Engineering Research Council of Canada. We are extremely grateful to B. Whittaker and K. M. Glover of Atomic Energy Research Establishment Harwell for supplying the ^{235}Np source.

[1]O. Beckman, Ark. Phys. 9, 495 (1955).
[2]J. H. Scofield, Phys. Rev. 179, 9 (1969).
[3]S. I. Salem, S. L. Panossian, and R. A. Krause, At. Data Nucl. Data Tables 14, 91 (1974).
[4]J. H. Scofield, Phys. Rev. A 9, 1041 (1974).
[5]J. L. Campbell and C. W. Schulte, Phys. Rev. A 22, 609 (1980).
[6]G. Barreau, H. G. Börner, T. von Egidy, and R. W. Hoff, Z. Phys. A 308, 219 (1982).
[7]E. G. Kessler, Jr., R. D. Deslattes, D. Girard, W. Schwitz, L. Jacobs, and O. Renner, Phys. Rev. A 26, 2696 (1982).
[8]O. W. B. Schult, Z. Naturforsch., Teil A 26, 368 (1971).
[9]S. I. Salem, B. G. Saunders, and G. C. Nelson, Phys. Rev. A 1, 1563 (1970).
[10]G. C. Nelson and B. G. Saunders, Phys. Rev. 188, 108 (1969).
[11]A. G. de Pinho, Phys. Rev. A 3, 905 (1971).
[12]P. F. Dittner and C. E. Bemis, Jr., Phys. Rev. A 5, 481 (1972).
[13]P. R. Bevington, *Data Reduction and Error Analysis for the Physical Sciences* (McGraw-Hill, New York, 1971).
[14]J. L. Campbell, Int. J. Appl. Radiat. Isot. 33, 661 (1982).
[15]B. H. Armstrong, J. Quant. Spectrosc. Radiat. Transfer 7, 61 (1976).
[16]*Table of Isotopes*, 7th ed., edited by C. M. Lederer and V. S. Shirley (Wiley, New York, 1978).
[17]G. F. Knoll, *Radiation Detection and Measurement* (Wiley, New York, 1979).
[18]M. O. Krause and J. H. Oliver, J. Phys. Chem. Ref. Data 8, 329 (1978).
[19]T. Sekine and H. Baba, Nucl. Instrum. Methods 133, 171 (1976).
[20]J. H. Scofield, At. Nucl. Data Tables 14, 121 (1974).